ISSN 1070-3284, Russian Journal of Coordination Chemistry, 2016, Vol. 42, No. 2, pp. 96–103. © Pleiades Publishing, Ltd., 2016.

Syntheses, Crystal Structures, and Properties of Three Two-Dimensional Complexes Constructed by Flexible (2,3-Pyridylmethyl)amine[1]

C. M. Yue, D. Z. Gao*, and X. G. Wang

Tianjin Key Laboratory of Structure and Performance for Functional Molecules,
Key Laboratory of Inorganic-Organic Hybrid Functional Material Chemistry, Ministry of Education,
College of Chemistry, Tianjin Normal University,
Tianjin, 300387 P.R. China
**e-mail: tjgaodz@sina.com*

Received May 7, 2015

Abstract—Three two-dimensional coordination polymers $[Cd(2,3\text{-Pyma})Cl_2]_n$ (**I**), $\{[Cd(2,3\text{-Pyma})(1,4\text{-Chdc})] \cdot 4H_2O\}_n$ (**II**) and $\{[Zn_2(2,3\text{-Pyma})(1,2,4,5\text{-Bttc})(H_2O)_4] \cdot 6H_2O\}_n$ (**III**) (2,3-Pyma = (2,3-pyridylmethyl)amine, H_2-1,4-Chdc = 1,4-cyclohexanedicarboxylic acid, and H_4-1,2,4,5-Bttc = 1,2,4,5-benzenetetracarboxylic acid) have been synthesized and structurally characterized by single crystal X-ray crystallography (CIF files CCDC nos. 989461 (**I**), 1055685 (**II**) and 1055686 (**III**)). Three complexes are all two-dimensional layer networks bridged by the flexible 2,3-Pyma ligands or the carboxylate ligands. It is noted that the flexible 1,4-Chdc ligands bind the Cd^{2+} ions into a helical chain structure in complex **II**. The photoluminescence and thermal properties are investigated.

DOI: 10.1134/S107032841602010X

INTRODUCTION

During the past decade, considerable efforts have been devoted to construct new metal–organic coordination polymers (MOCPs), not only owing to their enormous variety of intriguing structural topologies but also because of their great potential applications as microporous, magnetic and fluorescent materials [1–3]. An effective and facile approach for the synthesis of such complexes is still the self-assembly of well-designed multi-dentate organic ligands and *d*-block (or *f*-block) metal ions under hydrothermal conditions [4, 5]. However, many factors, such as the coordination geometry of the central metal ion, the organic ligands and counterions, as well as the synthetic methods, all influence the structure of the MOCPs [6, 7]. The selection of the suitable ligands always plays an important role in the determining the topologies and properties of these coordination networks. Recently, the MOCPs constructed from divalent d^{10} configuration ions have attracted high levels of interest because of their potential to serve in hydrogen storage, gas absorption, photoluminescence and nonlinear optical applications [8–10]. In order to construct more complicated and fantastic MOCPs, the combination of the pyridine-based ligands and the multicarboxylates as mixed ligands has been widely used to meet the coordination geometry requirement of the d^{10} configuration ions [11–13]. In this paper, we select a new flexible pyridine-based ligand (2-pyridylmethyl,3-pyridylmethyl)amine (2,3-Pyma) [14] and two auxiliary multicarboxylate ligands (1,4-Chdc [15, 16] and 1,2,4,5-Bttc [17, 18]) to construct polymeric architectures due to their variety of bridging abilities. Herein we report three two-dimensional coordination polymers $[Cd(2,3\text{-Pyma})Cl_2]_n$ (**I**), $\{[Cd(2,3\text{-Pyma})(1,4\text{-Chdc})] \cdot 4H_2O\}_n$ (**II**) and $\{[Zn_2(2,3\text{-Pyma})(1,2,4,5\text{-Bttc})(H_2O)_4] \cdot 6H_2O\}_n$ (**III**) bridged by 2,3-Pyma or carboxylate ligands.

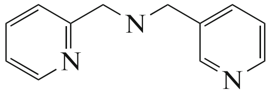

(2,3-Pyma ligand)

EXPERIMENTAL

Material and instruments. All chemicals were of reagent grade and used without purification. The 2,3-Pyma ligand was prepared according to the literature method [19]. Elemental analyses for carbon, hydrogen and nitrogen were carried out on a Leeman-Labs CE-440 elemental analyzer. The infrared spectra were taken on a Nicolet Avatar 370 FT-IR spectrometer in the range of 4000–400 cm^{-1} by KBr pellet technique.

---

[1] The article is published in the original.

Solid-state luminescence spectra were recorded at room temperature on an F-4500 FL spectrophotometer. Thermogravimetric analyses (TGA) were performed on a Perkin-Elmer TGAQ 500 thermogravimetric analyzer under flowing N_2 atmosphere with a heating rate of 5°C min^{-1} up to 650°C.

Synthesis of complex I. $CdCl_2 \cdot 6H_2O$ (29.1 mg, 0.1 mmol) and 2,3-Pyma ligand (19.9 mg, 0.1 mmol) were dissolved in distilled water (15 mL) with constant stirring for 1 h and filtered at room temperature. After the filtrate was allowed to stand at room temperature for one week, colorless block crystals suitable for X-ray structure analysis were grown by the slow evaporation. The yield was ~31% based on $CdCl_2 \cdot 6H_2O$.

For $C_{12}H_{13}N_3Cl_2Cd$

anal. calcd., %:	C, 37.6;	H, 3.4;	N, 11.0.
Found, %:	C, 37.5;	H, 3.5;	N, 11.1.

IR spectrum (KBr; ν, cm^{-1}): 3199 s, 1438 m, 1111 m, 812 m, 618 m.

Synthesis of complex II. $CdCl_2 \cdot 6H_2O$ (29.1 mg, 0.1 mmol) and 2,3-Pyma ligand (19.9 mg, 0.1 mmol) were dissolved in distilled water (10 mL) with constant stirring for 1 h, followed by adding the aqueous solution (5 mL) of disodium 1,4-cyclohexanedicarboxylate (21.6 mg, 0.1 mmol) at room temperature. Then the mixture was stirred for 1 h and filtered. After the filtrate was allowed to stand at room temperature for one week, colorless block crystals suitable for X-ray structure analysis were grown by the slow evaporation. The yield was ~27% based on $CdCl_2 \cdot 6H_2O$.

For $C_{40}H_{62}N_6O_{16}Cd_2$

anal. calcd., %:	C, 43.3;	H, 5.6;	N, 7.6.
Found, %:	C, 43.4;	H, 5.5;	N, 7.7.

IR spectrum (KBr; ν, cm^{-1}): 3137 br, 1600 s, 1551 s, 1437 m, 1437 m, 1344 m, 1195 m, 1004 m, 889 m, 761 m.

Synthesis of complex III was carried out in the same procedure as described for complex **II** except that $ZnCl_2 \cdot 6H_2O$ and tetrasodium 1,2,4,5-benzenetetracarboxylate were used instead of $CdCl_2 \cdot 6H_2O$ and disodium 1,4-cyclohexanedicarboxylate. Colorless block crystals were grown at room temperature by the slow evaporation. The yield was ~23% based on $ZnCl_2 \cdot 6H_2O$.

For $C_{22}H_{35}N_3O_{18}Zn_2$

anal. calcd., %:	C 34.7;	H 4.6;	N 5.5.
Found, %:	C 34.8;	H 4.5;	N 5.6.

IR spectrum (KBr; ν, cm^{-1}): 3397 br, 1609 s, 1487 m, 1419 m, 1369 m, 1135 m, 821 m, 713 m, 618 m.

Structure determination. The block single-crystals of complexes **I** (0.18 × 0.17 × 0.16 mm), **II** (0.20 × 0.18 × 0.15 mm) and **III** (0.12 × 0.08 × 0.07 mm) were selected and mounted on glass fibers. The X-ray diffraction measurements of complexes **I** and **III** were collected on a Bruker APEX-II CCD diffractometer equipped with a graphite-monochromatic MoK_α radiation source ($\lambda = 0.71073$ Å), while that of complex **II** was detained on a Bruker CCD area detector diffractometer. The empirical adsorption corrections by SADABS were carried out. The structures were solved by direct methods using the SHELXS-97 program [20] and refined with SHELXL-97 [20] by full-matrix least-squares techniques on F^2. All non-hydrogen atoms were refined anisotropically, while the hydrogen atoms were located geometrically and refined isotropically. Details of the crystal parameters, date collection and refinements for three complexes are summarized in Table 1. Selected bond lengths and bond angles are listed in Table 2.

Crystallographic data (excluding structure factors) for the structures in this paper have been deposited with the Cambridge Crystallographic Data Centre (CCDC nos. 989461 (**I**), 1055685 (**II**) and 1055686 (**III**); deposit@ccdc.cam.ac.uk, http://www.ccdc.cam.ac.uk).

RESULTS AND DISCUSSION

The X-ray crystallography reveals that complex **I** consists of neutral two-dimensional (2D) layers. In the coordination environments as shown in Fig. 1a, there are crystallographically two unique Cd(II) centers in the asymmetric unit with the distorted octahedral coordination geometries. The Cd(1) ion is coordinated by two pyridine nitrogen atoms from two different 2,3-Pyma ligands and four chlorine anions, while the Cd(2) ion is coordinated by four nitrogen atoms from two different 2,3-Pyma ligands and two chlorine anions. The Cd–N bond lengths are in the range of 2.334(3) to 2.385(3) Å and the Cd–Cl bond distances vary from 2.6236(13) to 2.7215(15) Å, respectively. Meantime, each 2,3-Pyma ligand bridges two Cd^{2+} ions to afford one-dimensional (1D) chains, and the chlorine anions connect the chains to form an undulated 2D layer network with the (4,4) topology as shown in Fig. 2a.

Complex **II** contains neutral two-dimensional layers and free water molecules. In the coordination environment as depicted in Fig. 1b, there is one crystallographically unique Cd^{2+} ion which is six-coordinated in a distorted octahedral coordination geometry. The six sites of the Cd^{2+} ion are occupied by three nitrogen atoms from two different 2,3-Pyma ligands and three carboxyl oxygen atoms of two disparate 1,4-Chdc ligands, in which the bond lengths are in the range of

Table 1. Crystallographic data and structure refinements for complexes **I**–**III**

Parameter	Value		
	I	**II**	**III**
Fw	382.55	1107.76	760.27
Crystal system	Triclinic	Monoclinic	Triclinic
Space group	$P\bar{1}$	$P2_1$	$P\bar{1}$
a, Å	8.948(5)	8.9182(5)	9.729(3)
b, Å	9.100(5)	11.6124(6)	11.533(3)
c, Å	9.577(5)	11.3263(6)	14.459(4)
α, deg	67.293(8)	90	78.324(6)
β, deg	87.645(7)	90.6450(10)	79.376(6)
γ, deg	75.787(8)	90	76.129(6)
V, Å^3	696.1(6)	1172.90(11)	1526.6(7)
Z	2	1	2
ρ, g cm^{-3}	1.825	1.568	1.654
μ, mm^{-1}	1.937	0.980	1.656
F(000)	376	568	784
Crystal size, mm	0.18 × 0.17 × 0.16	0.20 × 0.18 × 0.15	0.12 × 0.08 × 0.07
θ Range for data collection, deg	2.31–25.01	1.80–25.01	1.45–25.01
Limiting indices	$-10 \leqslant h \leqslant 9$ $-10 \leqslant k \leqslant 6$ $-11 \leqslant l \leqslant 11$	$-10 \leqslant h \leqslant 10$ $-13 \leqslant k \leqslant 13$ $-13 \leqslant l \leqslant 6$	$-10 \leqslant h \leqslant 11$ $-13 \leqslant k \leqslant 13$ $-14 \leqslant l \leqslant 17$
Reflections collected/unique (R_{int})	3587/2423 (0.0182)	6075/3986 (0.0134)	7824/5357 (0.1049)
Completeness to θ = 25.01, %	98.5	100.0	99.4
Max and min transmission	0.7469 and 0.7219	0.8669 and 0.8281	0.8929 and 0.8261
Data/restraints/parameters	2423/0/166	3986/1/290	5357/6/418
Goodness-of-fit on F^2	1.035	1.005	1.004
Final R indices ($I > 2\sigma(I)$)	$R_1 = 0.0302$ $wR_2 = 0.0704$	$R_1 = 0.0216$ $wR_2 = 0.0496$	$R_1 = 0.0895$ $wR_2 = 0.1579$
R indices (all data)	$R_1 = 0.0360$ $wR_2 = 0.0749$	$R_1 = 0.0239$ $wR_2 = 0.0508$	$R_1 = 0.2114$ $wR_2 = 0.2069$
Largest diff. peak and hole, e Å^{-3}	0.886 and –0.506	0.618 and –0.254	0.918 and –0.683

Table 2. Selected bond lengths (Å) and bond angles (ω) for complexes **I–III***

Bond	*d*, Å	Bond	*d*, Å
I			
Cd(1)–N(3*A*)	2.334(3)	Cd(2)–N(1)	2.385(3)
Cd(1)–Cl(1)	2.7214(15)	Cd(1)–Cl(2)	2.6236(13)
Cd(2)–N(2)	2.363(3)	Cd(2)–Cl(1)	2.6601(13)
II			
Cd(1)–O(2)	2.268(2)	Cd(1)–N(1)	2.308(2)
Cd(1)–N(3*A*)	2.333(3)	Cd(1)–O(3*B*)	2.344(2)
Cd(1)–N(2)	2.432(2)	Cd(1)–O(4*B*)	2.491(2)
III			
Zn(1)–O(5)	1.947(7)	Zn(1)–O(7*A*)	1.967(7)
Zn(1)–O(1)	1.973(7)	Zn(1)–N(3)	2.044(9)
Zn(2)–O(11)	2.037(8)	Zn(2)–O(12)	2.078(8)
Zn(2)–O(10)	2.087(8)	Zn(2)–N(1)	2.091(9)
Zn(2)–O(9)	2.145(9)	Zn(2)–N(2)	2.189(11)
Angle	ω, deg	Angle	ω, deg
I			
N(3*B*)Cd(1)Cl(2)	88.77(8)	Cl(2)Cd(1)Cl(1*C*)	94.57(3)
N(3*A*)Cd(1)Cl(1)	89.13(8)	N(2*D*)Cd(2)N(1)	107.06(10)
N(3*A*)Cd(1)Cl(1*C*)	90.87(8)	N(2)Cd(2)Cl(1)	87.84(8)
N(2)Cd(2)N(1)	72.94(10)	N(1)Cd(2)Cl(1)	90.27(8)
Cl(2)Cd(1)Cl(1)	85.43(3)		
II			
O(2)Cd(1)N(1)	95.64(8)	O(2)Cd(1)N(3*A*)	88.47(8)
N(1)Cd(1)N(3*A*)	168.63(8)	O(2)Cd(1)O(3*B*)	85.92(8)
N(1)Cd(1)O(3*B*)	98.58(9)	N(3*A*)Cd(1)O(3*B*)	92.28(9)
O(2)Cd(1)N(2)	140.56(8)	N(1)Cd(1)N(2)	73.09(8)
N(3*A*)Cd(1)N(2)	97.05(8)	O(3*B*)Cd(1)N(2)	132.50(8)
O(2)Cd(1)O(4*B*)	138.58(8)	N(1)Cd(1)O(4*B*)	98.48(9)
N(3*A*)Cd(1)O(4*B*)	85.22(9)	O(3*B*)Cd(1)O(4*B*)	53.59(8)
N(2)Cd(1)O(4*B*)	80.86(8)		
III			
O(5)Zn(1)O(7*A*)	109.3(3)	O(5)Zn(1)O(1)	105.3(3)
O(7*A*)Zn(1)O(1)	124.4(3)	O(5)Zn(1)N(3)	107.7(3)
O(7*A*)Zn(1)N(3)	99.3(3)	O(1)Zn(1)N(3)	110.0(3)
O(11)Zn(2)O(12)	93.7(4)	O(11)Zn(2)O(10)	90.4(3)
O(12)Zn(2)O(10)	86.6(3)	O(11)Zn(2)N(1)	172.5(4)
O(12)Zn(2)N(1)	91.6(4)	O(10)Zn(2)N(1)	95.2(4)
O(11)Zn(2)O(9)	90.4(4)	O(12)Zn(2)O(9)	174.1(4)
O(10)Zn(2)O(9)	89.1(3)	N(1)Zn(2)O(9)	84.6(4)
O(11)Zn(2)N(2)	94.3(4)	O(12)Zn(2)N(2)	86.7(4)
O(10)Zn(2)N(2)	172.1(3)	N(1)Zn(2)N(2)	80.7(4)
O(9)Zn(2)N(2)	97.2(4)		

* Symmetry transformations used to generate equivalent atoms: for **I** (*A*) $-x + 1, -y, -z + 1$; (*B*) $x, y + 1, z$; (*C*) $-x + 1, -y + 1, -z + 1$; (*D*) $-x + 1, -y + 1, -z$; for **II** (*A*) $-x + 2, y - 1/2, -z + 1$; (*B*) $-x + 2, y - 1/2, -z + 2$; for **III** (*A*) $-x, -y + 1, -z + 1$.

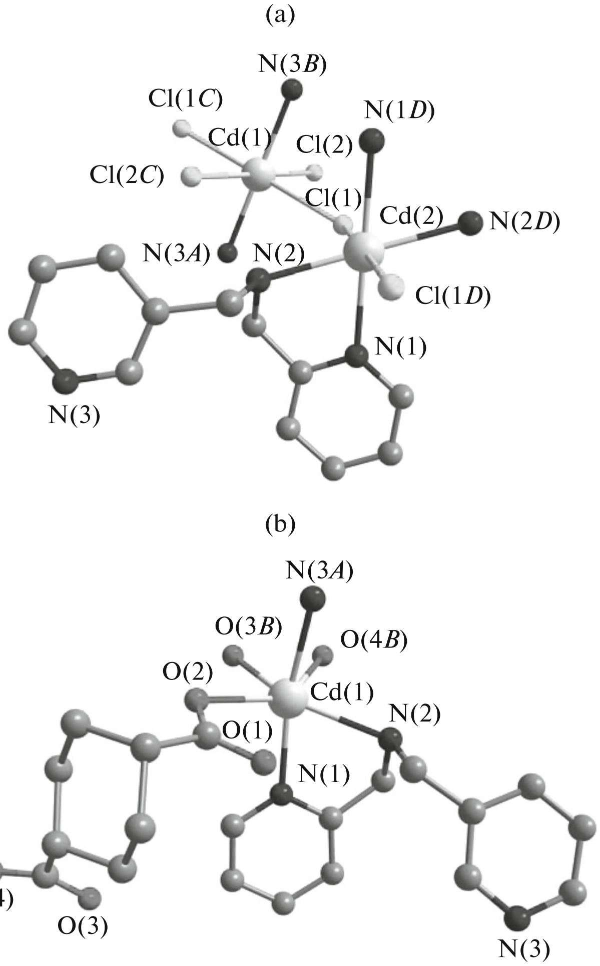

Fig. 1. View of the coordination environment of the Cd(II) centers in complexes **I** (a) and **II** (b). Hydrogen atoms are omitted for clarity.

2.268(2) to 2.491(2) Å. Each 2,3-Pyma ligand connects two Cd^{2+} ions to afford one-dimensional (1D) chains and the 1,4-Chdc ligands further link the 1D chains to generate an undulated 2D layer network with the (4,4) topology as depicted in Fig. 2b. In the two-dimensional layer, the Cd–Cd distances mediated by the 2,3-Pyma and 1,4-Chdc ligands are 8.4981(4) and 7.7843(4) Å, respectively. It is noteworthy that the flexible 1,4-Chdc ligands form the polymeric helical chains propagating along the crystallographic *y* axis with a helical pitch of 11.6124(6) Å as shown in Fig. 3.

Complex **III** also have a 2D layer structure, in which there are two crystallographic unique Zn^{2+} ions per asymmetric unit as illustrated in Fig. 4. The local coordination geometry around the Zn(1) center can be described as a slightly distorted tetrahedral configuration including three carboxyl oxygen atoms of three disparate 1,2,4,5-Bttc ligands and one pyridyl nitrogen atom from 2,3-Pyma. Each Zn(2) ion is six-coordinated with a distorted octahedron fashion coordinated by four water oxygen atoms and two nitrogen atoms from 2,3-Pyma ligands. The bond lengths around the Zn(II) centers vary from 1.947(7) to 2.189(11) Å. It should be noted that the auxiliary 1,2,4,5-Bttc ligands adopt two different binding fashions. Half of the 1,2,4,5-Bttc ligands as tetra-unidentate mode bridge Zn(1) ions to afford 1D chains, and the other half ones as bis-unidentate mode further link the chains to generate 2D layer networks as shown in Fig. 5. When half of the 1,2,4,5-Bttc ligands are as linear linkers and the other half ones are taken as four-coordinated nodes as well as the Zn(II) centers as planar three-coordinated nodes, the whole 2D sheet can thus be represented topologically by Schläfli symbol $\{4.6^2\}_2\{4^2.6^2.8^2\}$ as illustrated in Fig. 5. In addition, the moieties of Zn(2) ions and the coordinated 2,3-Pyma ligands are outspread at both sides of the 2D layers as terminal pendent arms.

Luminescent coordination complexes have attracted great attention because of their potential applications as chemical sensors, photochemistry and electroluminescence displays [21, 22]. To study the

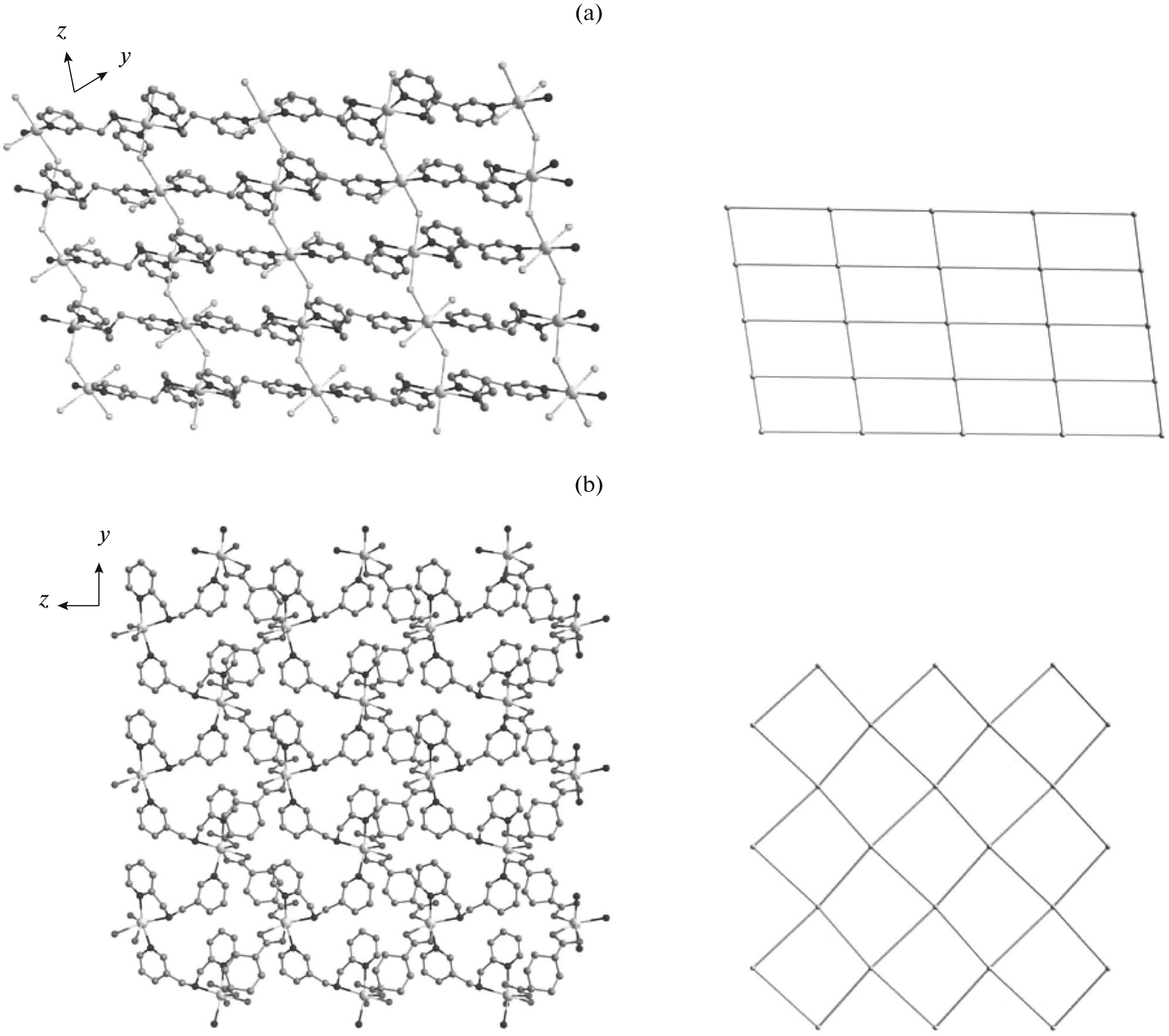

Fig. 2. View of the 2D layer network of complexes **I** (a) and **II** (b) parallel to the *yz* plane (left); schematic illustrating the (4,4) topology for complexes **I** (a) and **II** (b) (right).

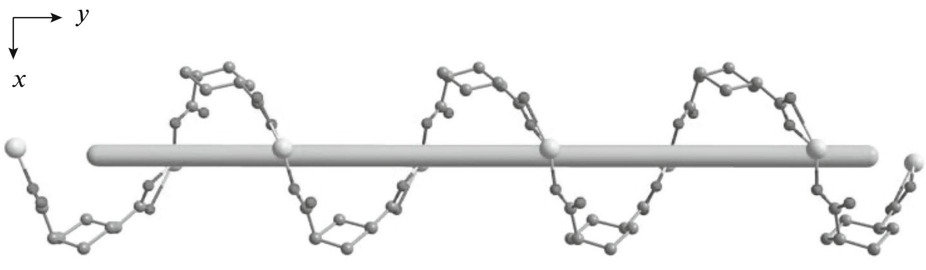

Fig. 3. A perspective view of the one-dimensional helical chain structure along the *y* axis in complex **II**.

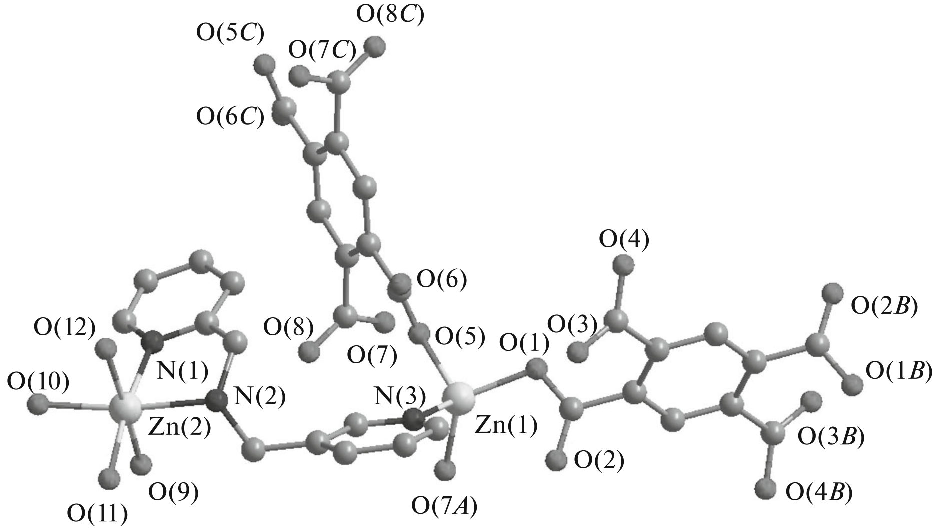

Fig. 4. View of the coordination environment of the Zn(II) centers in complex **III** (symmetry code: (*A*) $-x, -y + 1, -z + 1$; (*B*) $-x, -y + 1, -z$; (*C*) $-x + 1, -y + 1, -z + 1$). Hydrogen atoms and lattice water molecules are omitted for clarity.

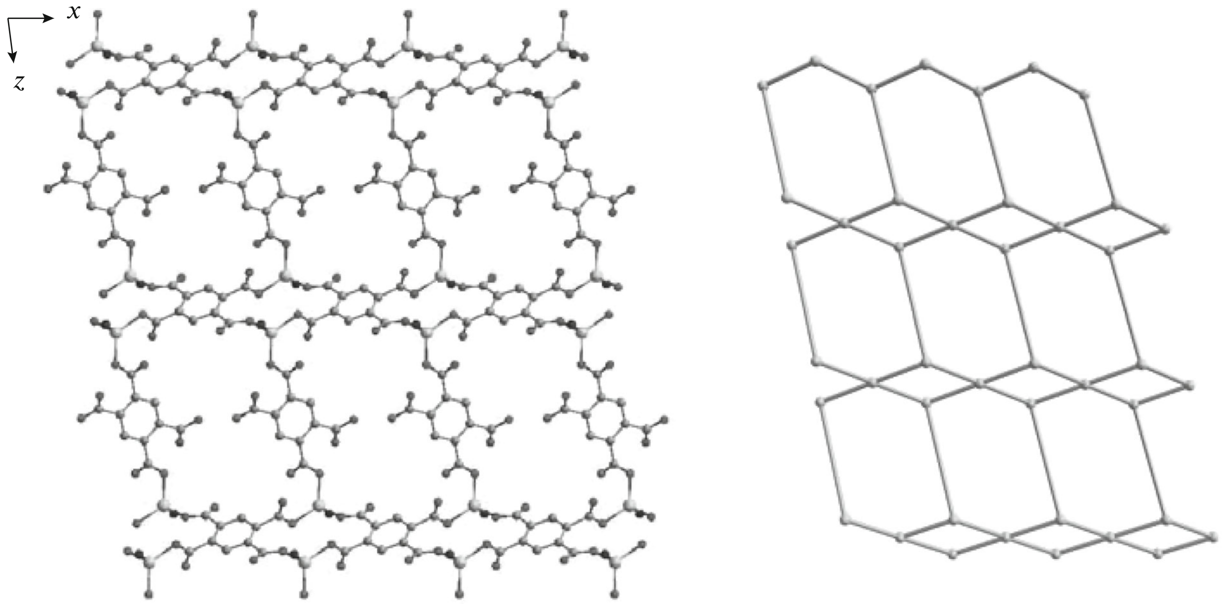

Fig. 5. View of the 2D layer network of complex **III** parallel to the *xz* plane (left; the Zn(2) ions and 2,3-Bpma ligands are omitted for clarity); schematic illustrating the $\{4.6^2\}_2\{4^2.6^2.8^2\}$ topology for complex **III** (right).

fluorescent properties of complexes **II** and **III**, the emission spectra were recorded in the solid state at ambient temperature, which are depicted in Fig. 6. It can be seen that the peak of the weak emission band for complex **II** is located at 475 nm (λ_{ex} = 365 nm), while complex **III** exhibits intense photoluminescence emission band with the peaks at 442 and 474 nm (λ_{ex} = 300 nm). According to the reported literatures, there are no intense fluorescent emissions for the free 2,3-Pyma [14] and 1,4-Chdc ligands [23] at the excitation wavelengths between 240 and 540 nm under the same experimental conditions, whereas the 1,2,4,5-Bttc ligand produces a fluorescence emission band with the maximum peak at 393 under 347 nm excitation [24]. Therefore, the intense fluorescent emission for complex **III** should be proposed to the intraligand $\pi \rightarrow \pi^*$ transfer of the 1,2,4,5-Bttc ligand. The slight red-shift of the emission band may be attributed to the coordination of the 1,2,4,5-Bttc ligand to metal ions. This

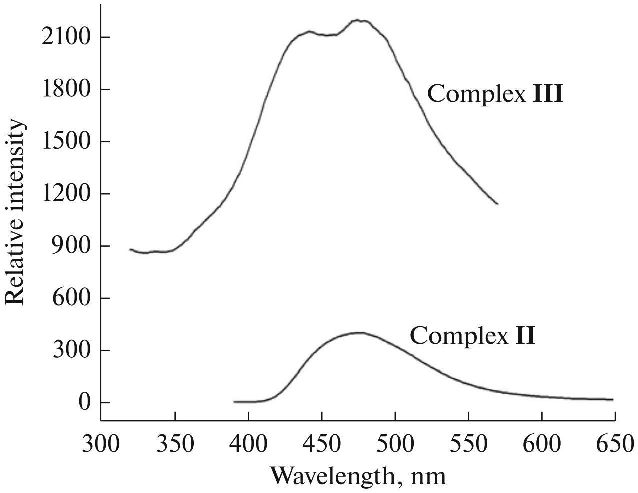

Fig. 6. Solid-state fluorescence emissions recorded at room temperature for complexes **II** and **III**.

suggests that complex **III** may be a good candidate for potential hybrid inorganic-organic photoactive materials.

All the synthesized complexes are air stable. TGA experiments for three complexes were carried out to examine the thermal stability. The TGA curves of complexes **I** and **II** show a gradual release in the temperature range 15–250°C, indicating the exclusion of lattice water molecules and the surface absorption of moisture. The obvious decomposition of the whole structure is observed from about 170°C for complex **I** and 250°C for complex **II**. Complex **III** exhibits a two-step weight loss process including the first obvious weight loss of 23.2% from 15 to 100°C attributed to the exclusion of all water molecules (calcd. 23.7%), and the second vigorously framework collapse at temperature higher than 300°C.

REFERENCES

1. Keeffe, M.O., Peskov, M.A., Ramsden, S.J., and Yaghi, O.M., *Acc. Chem. Res.*, 2008, vol. 41, p. 1782.
2. Perry, J.J., Perman, J.A., and Zaworotko, M.J., *Chem. Soc. Rev.*, 2009, vol. 38, p. 1400.
3. Harbuzaru, B.V., Corma, A., Rey, F., et al., *Angew. Chem. Int. Ed.*, 2009, vol. 48, p. 6476.
4. Stock, N. and Biswas, S., *Chem. Rev.*, 2012, vol. 112, p. 933.
5. Hou, Y.L., Xia, H., Cheng, R.R., and Zhao, B., *Chem. Commun.*, 2015, vol. 51, p. 6769.
6. Ghosh, A.K., Ghoshal, D., Zangrando, et al., *Inorg. Chem.*, 2007, vol. 46, p. 3057.
7. Yang, J., Ma, J.F., Liu, Y.Y., et al., *Cryst. Growth Des.*, 2009, vol. 9, p. 1894.
8. Xu, X., Lu, Y., Wang, E., et al., *Cryst. Growth Des.*, 2006, vol. 6, p. 2029.
9. Rowsell, J.L.C. and Yaghi, O.M., *J. Am. Chem. Soc.*, 2006, vol. 128, p. 1304.
10. Shu, Y.B., Tu, N., Shi, H.T., et al., *Dalton Trans.*, 2015, vol. 44, p. 7131.
11. Zhang, J., Chen, Y.B., Chen, S.M., et al., *Inorg. Chem.*, 2006, vol. 45, p. 3161.
12. Liu, F.J., Hao, H.J., Sun, C.J., et al., *Cryst. Growth Des.*, 2012, vol. 12, p. 2004.
13. Ju, Z.M., Cao, D.P., Qin, L., et al., *CrystEngComm*, 2014, vol. 16, p. 3917.
14. Xi, P.M., Wang, S.S., Gao, D.Z., et al., *Transition. Met. Chem.*, 2013, vol. 38, p. 873.
15. Kumagai, H., Akita-Tanaka, M., Inoue, K., et al., *Inorg. Chem.*, 2007, vol. 46, p. 5949.
16. Ge, Y., Li, N.Y., Ma, W., et al., *CrystEngComm*, 2014, vol. 16, p. 10949.
17. Gang, Y., Shao, K.Z., Du, D.Y., et al., *CrystEngComm*, 2012, vol. 14, p. 1865.
18. Shen, J.J., Li, M.X., Wang, Z.X., et al., *Cryst. Growth Des.*, 2014, vol. 14, p. 2818.
19. Soibinet, M., Dechamps-Olivier, I., Mohamadou, A., and Aplincourt, M., *Inorg. Chem. Commun.*, 2004, vol. 7, p. 405.
20. Sheldrick, G.M., *Acta Crystallogr., Sect. A: Found. Crystallogr.*, 2008, vol. 64, p. 112.
21. Zhao, B., Chen, X.Y., Cheng, P., et al., *J. Am. Chem. Soc.*, 2004, vol. 126, p. 15394.
22. Manbeck, G.F., Brennessel, W., Evans, C.M., and Eisenberg, R., *Inorg. Chem.*, 2010, vol. 49, p. 2834.
23. Yang, E.C., Zhao, H.K., Ding, B., et al., *Cryst. Growth Des.*, 2007, vol. 7, p. 2009.
24. Hou, Y., Wang, S.T., Shen, E., et al., *Inorg. Chim. Acta*, 2004, vol. 357, p. 3155.